Unimolecular Dissociation of Formyl Halides HXCO → CO + HX (X= F, Cl): An Ab Initio Direct Classical Trajectory Study

Smriti Anand and H. Bernhard Schlegel*

Department of Chemistry and Institute of Scientific Computing, Wayne State University, Detroit, Michigan 48202

Received: June 26, 2002

The dynamics of the unimolecular dissociation of formyl halides, HXCO (X = F, Cl), have been studied by classical trajectory calculations at the MP2/6-31G(d,p) level of theory and have been compared to similar calculations for H_2CO. The calculated transition states are planar with elongated C−X and H−X bonds. Trajectories were started from the transition state with 12 kcal/mol of energy above the potential barrier, corresponding to the zero-point energy plus 2.25 and 2.87 kcal/mol of excess energy in the transition vector of formyl fluoride and formyl chloride, respectively. The CO fragments are produced rotationally hot with $\langle J \rangle = 40-50$ but vibrationally cold with only 10−20% in $v = 1$. The HX fragment shows significant vibrational excitation with $\langle v \rangle = 1.0$ for HF and $\langle v \rangle = 2.3$ for HCl, compared to $\langle v \rangle = 1.16$ for H_2. The average rotational quantum number for HCl, $\langle J \rangle = 12.8$, is considerably higher than for HF, $\langle J \rangle = 9.5$, or H_2, $\langle J \rangle = 3.3$. Product translation receives about 42% of the available energy in formyl fluoride and about 31% in formyl chloride compared to 70% for formaldehyde. The results show good qualitative agreement with the available experimental energy partitioning for HFCO; HF is observed to be vibrationally hot, but the distribution has not been measured. No experiments are available for HClCO dissociation.

Introduction

The unimolecular dissociation dynamics of small molecules is of interest to both experimentalists and theoreticians. The mode specificity of the reactants, the reaction threshold, and the distribution of energy in the products are some of the details that are studied. In this respect, the photodissociation of formaldehyde (H_2CO) has been studied extensively by experiment[1−13] and theory.[14−29] Formyl fluoride (HFCO)[30−47] and formyl chloride (HClCO)[36,48,49] have received much less attention. These fluorine- and chlorine-substituted analogues of H_2CO are formed in the degradation of hydrochlorofluorocarbons (HCFC).[50,51] The photodissociation of these halogenated molecules is of importance, as their degradation has important consequences for the earth's protective ozone layer.[52−54] The various dissociation routes for HXCO are

$$\mathrm{HXCO} \rightarrow \mathrm{H} + \mathrm{XCO} \quad (1)$$

$$\rightarrow \mathrm{X} + \mathrm{HCO} \quad (2)$$

$$\rightarrow \mathrm{HX} + \mathrm{CO} \quad (3)$$

$$\rightarrow \mathrm{XCOH} \quad (4)$$

$$\rightarrow \mathrm{HCOX} \quad (5)$$

Of these pathways, the molecular dissociation channel (reaction 3) is found to be the lowest-energy path.

Studies by Choi and Moore[30−33] have shown that stimulated emission pumping can prepare formyl fluoride (HFCO) in a specific dissociative level in the ground electronic state, where it dissociates to HF + CO. HFCO is excited to the S_1 state and is then stimulated to emit to a vibrationally excited level of the ground state, which can dissociate.[30,33] They observed that the intramolecular vibrational redistribution (IVR) was mode-specific in the energy region where it dissociates, with high overtone states of out-of-plane bending being exceptionally stable.[31] Measurements of the unimolecular dissociation rates showed that there is a large change in the rate for a small change in the rovibrational state.[32] The dissociation rate was found to increase by a factor of 10 to 100 or more for a small increase in the rotational quantum number from $J = 0$ to $J = 4$ and also exhibited mode specificity. The barrier for the dissociation was measured to be 49 ± 4 kcal/mol from these rates. Saito et al. studied the thermal decomposition of HFCO in shock waves and deduced a barrier height of 43 kcal/mol.[43] Moore et al. have also studied the CO rotational distribution and Doppler width.[34] They found that the CO fragment is rotationally hot and that the rotational distribution is significantly different for different initial states. About 20% of the available energy goes into the CO rotation, and 50% goes into product translation. The internal energy of the HF fragment accounts for the remaining 30% of the energy. As early as 1973, Klimek and Berry[55] found that photolysis of HFCO leads to HF laser emission. The average vibrational energy of HF was estimated to be about 10 ± 3 kcal/mol, which is ≈7% of the available energy. In an infrared multiphoton decomposition (IRMPD) study of HFCO, Ishikawa, Sugita, and Arai[44] found that CO was produced in its ground vibrational state while HF was produced vibrationally hot.

Formyl fluoride has also been the subject of several theoretical studies. Morokuma, Kato, and Hirao[38] initially studied the ground-state potential energy surface (PES) of HFCO by ab initio methods at the HF/4-31G level of theory. They calculated the transition state, barrier height, and intrinsic reaction coordinate for the molecular dissociation of HFCO. The transition state for the dissociation was found to be planar, with a barrier of 58 kcal/mol. Subsequently, Morokuma and Kamiya[37] carried out studies at a higher level of theory and estimated the

* Corresponding author. E-mail: hbs@chem.wayne.edu.

10.1021/jp021495c CCC: $22.00
Published on Web 10/29/2002

barrier height to be 46.9 kcal/mol at the MP4/6-311G**//MP2/6-31G* level. They located other stationary points on the PES including the transition state, complexes, and products for rearrangement and dissociation. Goddard and Schaefer[35] also studied the unimolecular dissociation and rearrangement of HFCO. Their estimate of the barrier height for the molecular dissociation was 47 kcal/mol using the coupled-cluster single and double method with the triple-ζ plus double-polarized basis set (CCSD TZ+2P). They confirmed the existence of singlet cis and trans fluorohydroxymethylenes and calculated the transition state for the isomerization reaction. Francisco and Zhao[36] studied the various reaction pathways for the decomposition of HFCO. At the PMP4/6-311++G(d,p) level of theory, they calculated the barrier height for the molecular dissociation (reaction 3) to be 43 kcal/mol compared to 94.4 kcal/mol for the C−H bond dissociation (reaction 1), 109.5 kcal/mol for the C−F bond dissociation (reaction 2), and 45 kcal/mol for isomerization to fluorohydroxycarbene (reaction 4). The thermochemistry of formyl halides has also been studied by Glukhovstev and Bach using the G2 theory.[47]

A number of analytical global PESs for this molecular dissociation have been constructed for use in dynamics calculations. Wei and Wyatt[39] carried out calculations at the MP4(SDTQ)/VTZ level and fitted the energies of nearly 4000 different geometries to two types of analytical functions—a high-order polynomial expansion using Simons−Parr−Filan (SPF) coordinates and a many-body expansion function. Their estimate of the barrier height was ≈45 kcal/mol. Budenholzer and Yu[46] performed classical trajectory calculations on a modified version of the Wei and Wyatt potential surface. They integrated about 6000 trajectories starting from the equilibrium geometry of HFCO by placing zero-point energy in each of the normal modes and then exciting a single normal mode such that the total energy was between 68.7 and 73.4 kcal/mol. They found clear evidence of mode specificity as the excitation of different modes gave significantly different reaction rates. Yamamoto and Kato[40] developed a new and more accurate ground-state PES at the MP2/cc-pVTZ level using about 4000 ab initio potential energies and fitting it to an analytical function composed of three local potential functions. Using this PES, they also carried out two types of classical trajectory studies. First, power spectra were calculated to investigate the intramolecular dynamics. Second, to study the energy partitioning between the HF and CO products, around 30 000 trajectories were initiated near the transition state, with each trajectory having a fixed energy of 12 kcal/mol above the potential energy of the transition state. The same authors also carried out a quantum dynamics study of the dissociation rates[41] and the mode specificity[42] of the unimolecular dissociation of HFCO on the modified PES. They observed large fluctuations in the time-dependent rate coefficients with the total energy and found that the coupling of the out-of-plane bending state with other in-plane vibrational states is weak.

Compared to the number of studies on H_2CO and HFCO, there have been very few studies on HClCO. The reaction pathways for the dissociation of HClCO on the ground-state PES have been studied by ab initio methods.[36] The barrier height was computed to be 37.8 kcal/mol at the PMP4/6-311++G(d,p) level of theory. Bent et al.[48] have carried out quantum chemistry and density functional calculations to compare with the experimental value of the vertical excitation energy of HClCO. The results of their density functional calculations (using a double numerical basis set with polarization) were in better agreement with experiment except for the most extensive quantum chemistry method used. Fang and Liu[49] have carried out ab initio studies on the lowest three electronic states of HClCO (S_0, S_1, and T_1) using the complete active space self-consistent field (CASSCF) and single- and multireference MP2 methods. The same authors have also carried out similar calculations on HFCO[45] and have found significant differences in the dissociation mechanism of the two molecules. At 230−320 nm, both HFCO and HClCO are excited to the S_1 state from which there are three possible routes—internal conversion (IC) to the ground state, intersystem crossing (ISC) to the lowest triplet state, and dissociation on the S_1 surface. The C−Cl bond cleavage on the S_1 PES is the most probable mechanism for the dissociation of HClCO at 230−320 nm. However, in case of HFCO, ISC from S_1 to T_1 and subsequent dissociation to H + FCO on the T_1 surface is the dominant route for dissociation at 218−248 nm, whereas at wavelengths shorter than 233 nm, the F−C bond dissociation on the S_1 surface can also compete with the H−C bond dissociation.

In the present study, we have used ab initio trajectory calculations to study the dynamics of the unimolecular dissociation of HXCO on the ground-state potential energy surface. Electronic structure theory is used to compute the PES directly rather than fitting to an analytical form.[56] In particular, classical trajectories have been computed for HXCO → HX + CO at the MP2 level of theory using the 6-31G(d,p) basis set.

Method

All of the calculations were carried out with the development version of the Gaussian[57] series of programs. The geometries of the ground state and the transition state of formyl fluoride and formyl chloride were optimized at the following levels of theory: Hartree−Fock [HF/3-21G and HF/6-31G(d)], second-order Møller−Plesset perturbation theory[58] [MP2/6-31G(d), MP2/6-31G(d,p), and MP2/6-311G(d,p)], Becke's three-parameter hybrid density functional method[59−61] [B3LYP/6-31G(d)], and QCISD/6-311G(d,p) (quadratic configuration interaction with single and double excitations[62]). Accurate heats of reaction and barrier heights were calculated using the complete basis extrapolation techniques of Peterson and co-workers[63] using the CBS-APNO method for HFCO and the CBS-QB3 method for both HFCO and HClCO. The second-order method of Gonzalez and Schlegel[64,65] was used to calculate the mass-weighted steepest reaction paths.

A Hessian-based predictor−corrector method[66,67] was used to integrate the ab inito classical trajectories. The Hessian was updated for five steps before being recalculated analytically. Step sizes of 0.5, 0.25, and 0.125 amu$^{1/2}$ bohr were used for the calculations. The trajectories were stopped when the fragments were at least 8 bohr apart and the gradient of the potential between the fragments was less than 1×10^{-5} hartree/bohr. The time taken for the trajectories to be completed was about 90 fs for HFCO and about 110 fs for HClCO. The total energy was conserved to about 1×10^{-7} hartree in both cases when step sizes of 0.25 and 0.125 amu$^{1/2}$ bohr were used.

The initial conditions chosen for the trajectory calculations were similar to those used by Yamamoto and Kato.[40] The trajectories were started at the transition state with 2.25 kcal/mol of kinetic energy in the transition vector for HFCO and 2.87 kcal/mol of kinetic energy in the case of HClCO. Zero-point energy was put in all of the other vibrational modes. This corresponds to an energy of 12 kcal/mol above the transition-state potential energy of both molecules. The total angular momentum was set to zero. The phases of the vibrational coordinates were chosen randomly. About 200 trajectories were

TABLE 1: Optimized Geometries for the Ground State of HFCO[a]

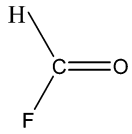

	C−O	C−F	C−H	F−C−O	H−C−O
HF/3-21G	1.179	1.347	1.072	122.3	127.7
HF/6-31G(d)	1.164	1.314	1.081	123.0	126.9
B3LYP/6-31G(d)	1.186	1.345	1.097	123.3	127.3
MP2/6-31G(d)	1.195	1.354	1.094	123.2	127.6
MP2/6-31G(d,p)	1.195	1.354	1.090	123.2	127.6
MP2/6-311G(d,p)	1.184	1.346	1.094	123.2	127.9
QCISD/6-311G(d,p)	1.180	1.342	1.096	123.0	127.7
MP2/cc-pVTZ[b]	1.184	1.348	1.085	123.0	127.9
CAS/cc-pVDZ[c]	1.184	1.330	1.091	122.8	128.0
experiment[d]	1.183	1.341	1.100	122.7	129.0

[a] Bond lengths in angstroms, angles in degrees. [b] Reference 40. [c] Reference 45. [d] Reference69.

TABLE 2: Optimized Geometries for the Ground State of HClCO[a]

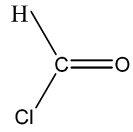

	C−O	C−Cl	C−H	Cl−C−O	H−C−O
HF/3-21G	1.171	1.892	1.072	122.3	131.3
HF/6-31G(d)	1.165	1.756	1.083	123.2	126.1
B3LYP/6-31G(d)	1.185	1.797	1.098	123.7	126.9
MP2/6-31G(d)	1.200	1.769	1.096	123.7	126.3
MP2/6-31G(d,p)	1.200	1.768	1.092	123.8	126.3
MP2/6-311G(d,p)	1.188	1.774	1.097	123.6	126.7
QCISD/6-311G(d,p)	1.185	1.774	1.097	123.5	126.3
MP2/cc-pVTZ[b]	1.189	1.768	1.092	123.7	126.5
CAS(14,10)/cc-pVDZ[b]	1.187	1.808	1.090	123.4	127.9
experiment[c]	1.182	1.765	1.090	123.1	126.5

[a] Bond lengths in angstroms, angles in degrees. [b] Reference 49. [c] Reference 70.

computed for each molecule at the MP2/6-31G(d,p) level of theory. Estimated error bars of one standard deviation were included in the appropriate plots.

The rotational quantum numbers of the diatomic products were calculated from the instantaneous angular momentum. For the analysis of the vibrational energy of the products, a Morse function was fitted to the potential energy at several distances. The vibrational quantum number was then calculated by integrating the momentum over one vibrational period according to the Einstein−Brillouin−Keller (EBK) semiclassical quantization condition.[68]

Results and Discussion

Structure and Energetics. The calculated geometric parameters for the ground states of formyl fluoride and formyl chloride are presented in Tables 1 and 2, respectively. These are in good agreement with previous calculations[36,37,40,45,49] and experiments.[69,70] The C−O and C−F bond lengths at the MP2/6-31G(d,p) level are about 0.01 Å longer than those in the QCISD/6-311G(d,p) calculations and the experimental values.[69] The C−O bond in HClCO is about 0.02 Å longer at the MP2/6-31G(d,p) level than in the CAS(14,10)/cc-pVDZ calculations and the experimental values.[70]

In Table 3 are collected the calculated geometric parameters for the transition state of formyl fluoride. The transition state is planar with long C−F and C−H bonds, in agreement with

TABLE 3: Optimized Geometries for the Transition State of HFCO[a]

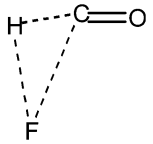

	C−O	C−F	C−H	H−F	O−C−F
HF/3-21G	1.131	1.782	1.135	1.345	122.8
HF/6-31G(d)	1.112	1.838	1.127	1.379	123.9
B3LYP/6-31G(d)	1.146	1.816	1.147	1.358	121.4
MP2/6-31G(d)	1.157	1.803	1.146	1.358	121.6
MP2/6-31G(d,p)	1.157	1.793	1.137	1.357	121.7
MP2/6-311G(d,p)	1.144	1.808	1.135	1.376	121.9
QCISD/6-311G(d,p)	1.136	1.823	1.133	1.392	122.2
MP2/cc-pVTZ[b]	1.140	1.843	1.126	1.389	122.2

[a] Bond lengths in angstroms, angles in degrees. [b] Reference 40.

TABLE 4: Optimized Geometries for the Transition State of HClCO[a]

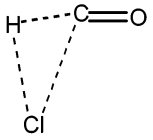

	C−O	C−Cl	C−H	H−Cl	O−C−Cl
HF/3-21G	1.116	2.552	1.104	1.982	126.6
HF/6-31G(d)	1.102	2.522	1.106	1.972	127.4
B3LYP/6-31G(d)	1.141	2.414	1.126	1.872	122.8
MP2/6-31G(d)	1.151	2.415	1.123	1.884	122.9
MP2/6-31G(d,p)	1.153	2.360	1.116	1.857	123.5
MP2/6-311G(d,p)	1.142	2.339	1.116	1.856	123.1
QCISD/6-311G(d,p)	1.133	2.355	1.116	1.876	123.7

[a] Bond lengths in angstroms, angles in degrees.

TABLE 5: Reaction Enthalpies and Barrier Heights for HFCO[a]

level	$\Delta H^{\ddagger}_{\text{forward},298}$	$\Delta H^{\circ}_{\text{r},298}$	$\Delta H^{\ddagger}_{\text{reverse},298}$
HF/3-21G	65.4	7	58.4
HF/6-31G(d)	68.4	1.3	67.0
B3LYP/6-31G(d)	54.1	18.1	36.0
MP2/6-31G(d)	54.1	7.2	46.9
MP2/6-31G(d,p)	52.8	4.3	48.5
MP2/6-311G(d,p)	50.3	−2.8	53.2
CBS-QB3	50.3	0.3	50.0
CBS-APNO	49.2	0.6	48.6
experiment	49 ± 4[b]	−1.5[c]	50.5 ± 4

[a] Enthalpies at 298 K in kcal/mol. [b] Reference 32. [c] Reference 71.

the calculations of Morokuma and co-workers.[38] At the transition state, the H−F distance is about 50% longer than the equilibrium HF bond length, suggesting that the product may be formed with considerable vibrational excitation. Similarly, the transition state for HClCO is also planar, and the H−Cl bond is about 48% longer than the equilibrium HCl bond length (see Table 4). The geometries of the transition states for HXCO → CO + HX (X= H, F, Cl) are best described as a 1,2 shift of X across the H−C bond of HCO. Population analysis shows that the migrating group has a partial negative charge (even for X = H), which is consistent with the greater stability of $X^- + HCO^+$ compared to $X^+ + HCO^-$. An alternative transition state involving the 1,2 shift of H^+ is disfavored because XCO^- is less stable toward dissociation than HCO^+.

The calculated barrier heights and heats of reaction are shown in Tables 5 and 6. The barriers computed for HFCO at CBS-QB3, 50.3 kcal/mol, and at CBS-APNO (our best level of theory), 49.2 kcal/mol, are both in good agreement with the experimental value of 49 ± 4 kcal/mol. Whereas the Hartree−

TABLE 6: Reaction Enthalpies and Barrier Heights for HClCO[a]

level	$\Delta H^{\ddagger}_{\text{forward},298}$	$\Delta H^{\circ}_{\text{r},298}$	$\Delta H^{\ddagger}_{\text{reverse},298}$
HF/3-21G	28.1	−10.4	58.4
HF/6-31G(d)	42.5	−10.2	67.0
B3LYP/6-31G(d)	37.9	7.4	36.0
MP2/6-31G(d)	42.7	1.5	46.9
MP2/6-31G(d,p)	40.9	−1.9	48.5
MP2/6-311G(d,p)	37.2	−6.4	53.2
CBS-QB3	37.4	−5.6	50.0

[a] Enthalpies at 298 K in kcal/mol

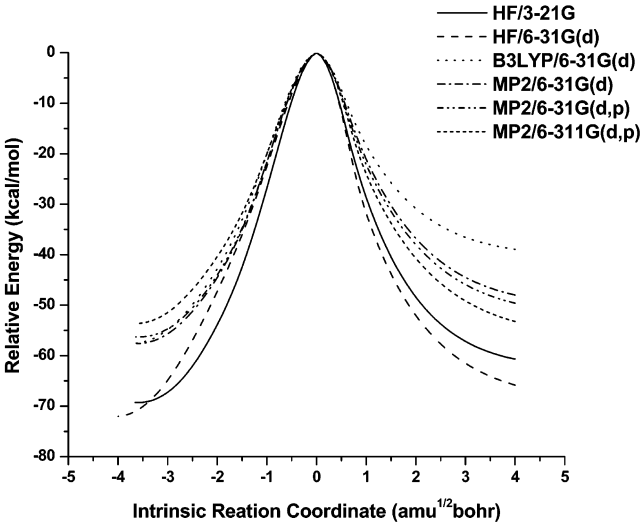

Figure 1. Potential energy along the reaction path for HFCO → HF + CO at HF/3-21G, HF/6-31G(d), B3LYP/6-31G(d), MP2/6-31G(d), MP2/6−31 g(d,p), and MP2/6-311G(d,p).

Fock level overestimates the barrier by about 16−19 kcal/mol, at all of the post SCF levels the barrier height is in good agreement with the experimental estimate. The MP2 level overestimates the barrier by about 1−4 kcal/mol. The experimental heats of reaction are calculated from the experimental heats of formation reported in the JANAF tables.[71] In the case of HClCO, our best estimate of the barrier height is the CBS-QB3 value of 37.4 kcal/mol. At all post SCF levels considered, the barrier height is within about 3 kcal/mol of the CBS-QB3 value. On the basis of the energy released in going from the transition state to the products, the MP2/6-31G(d,p) level of theory was chosen for the trajectory calculations as the best compromise between accuracy and affordability.

Potential Energy Profile. The potential energy profile along the mass-weighted steepest-descent reaction path (intrinsic reaction coordinate) of HFCO is shown in Figure 1. The energy released is too large by about 10−20 kcal/mol at the HF level of theory, about 12 kcal/mol too small at B3LYP, and differs by about ± 3 kcal at the MP2 level of theory when compared to the CBS-APNO calculations. In the formaldehyde case,[29] the energy released is about 20 kcal/mol too large at the HF level, about 1−3 kcal/mol too small at B3LYP, and about 10 kcal/mol too large at the MP2 level. The formation of the H−F bond is almost complete by about $s = 1.0$ amu$^{1/2}$ bohr. This corresponds to an H−F bond length of about 0.95 Å at MP2/6-31G(d,p). About 45% of the energy has been released at this point compared to 50% in the case of formaldehyde.[29] Figure 2 shows the potential energy profile along the reaction path for HClCO. At the HF level, the energy released is about 9−17 kcal/mol too large and about 14 kcal/mol too small at the B3LYP level compared to the CBS-QB3 value. The energy

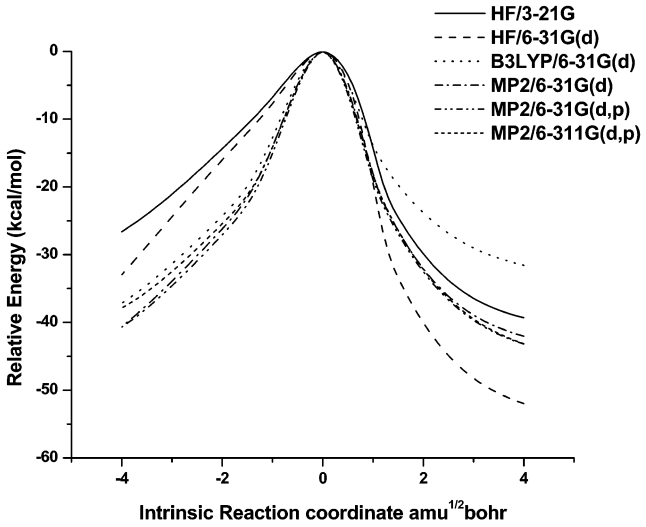

Figure 2. Potential energy along the reaction path for HClCO → HCl + CO at HF/3-21G, HF/6-31G(d), B3LYP/6-31G(d), MP2/6-31G(d), MP2/6−31 g(d,p), and MP2/6-311G(d,p).

TABLE 7: Vibrational Population of the Fragments at Various Step Sizes

		vibrational population in HFCO			vibrational population in HClCO	
step size		CO (%)	HF (%)		CO (%)	HCl (%)
	$v = 0$	74 ± 3	64 ± 3	$v = 0$	89 ± 2	2 ± 0.9
	$v = 1$	26 ± 3	36 ± 3	$v = 1$	11 ± 2	31 ± 3
0.5 amu$^{1/2}$ bohr[a]	$v = 2$			$v = 2$		41 ± 3
	$v = 3$			$v = 3$		19 ± 3
	$v = 4$			$v = 4$		8 ± 2
	$v = 0$	81 ± 3	29 ± 3	$v = 0$	88 ± 2	0
	$v = 1$	19 ± 3	42 ± 3	$v = 1$	12 ± 2	27 ± 3
0.25 amu$^{1/2}$ bohr[a]	$v = 2$		28 ± 3	$v = 2$		30 ± 3
	$v = 3$		1 ± 0.5	$v = 3$		33 ± 3
	$v = 4$			$v = 4$		10 ± 2
	$v = 0$	82 ± 3	30 ± 3	$v = 0$	88 ± 2	1 ± 0.6
	$v = 1$	18 ± 3	49 ± 3	$v = 1$	12 ± 2	20 ± 3
0.125 amu$^{1/2}$ bohr[b]	$v = 2$		19 ± 3	$v = 2$		35 ± 4
	$v = 3$		2 ± 1	$v = 3$		38 ± 4
	$v = 4$			$v = 4$		6 ± 2

[a] Two hundred trajectories each for HFCO and HClCO. [b] One hundred ninety trajectories for HFCO and 167 trajectories for HClCO.

released at the MP2 level differs by about ±4 kcal/mol. The formation of the H−Cl bond is about 90% complete by $s = 1.0$ amu$^{1/2}$ bohr, corresponding to an H−Cl bond length of 1.36 Å and an energy release of about 39% at the MP2/6-31G(d,p) level.

Effect of Step Size. At a step size of 0.5 amu$^{1/2}$ bohr, the trajectory calculations resulted in an energy conservation of only about 1×10^{-4} hartree. Because the reactions are complete in the first 40−60 fs and the vibrational frequency of the HX product is quite high, trajectory integrations with this large step size might actually be missing the important dynamics of the dissociation. In the case of HFCO, the vibrational population of HF did not show the expected degree of excitation, and the CO fragment was found to have more vibrational excitation than expected (Table 7). Step sizes of 0.25 amu$^{1/2}$ bohr and 0.125 amu$^{1/2}$ bohr resulted in better energy conservation (1×10^{-7} hartree) and gave product vibrational distributions in better agreement with earlier calculations.[40] At a step size of 0.25 amu$^{1/2}$ bohr, the vibrational distribution is statistically the same as the results from the 0.125 amu$^{1/2}$ bohr step size at a confidence level of 90%. In the case of HClCO, the vibrational distribution of CO did not vary significantly with step size. However, the HCl vibrational population peaked at $v = 2$ for s

TABLE 8: Vibrational Distribution of the Products

		CO		HX				
reaction	method	$v = 0$	$v = 1$	$v = 0$	$v = 1$	$v = 2$	$v = 3$	$v = 4$
$H_2CO \rightarrow H_2 + CO$	MP2/6-311G(d,p)[b]	87	13	30	34	27	10	
	experiment	88	12	24	41	25	9	
$HFCO \rightarrow HF + CO$	MP2/6-31G(d,p)[a,c]	81	19	29	45	24	1	
	Yamamoto and Kato[d]	83	17	17	45	33	5	
$HClCO \rightarrow HCl + CO$	MP2/6-31G(d,p)[a,c]	88	12	0	24	32	35	8

[a] Data from step sizes of 0.25 and 0.125 amu$^{1/2}$ bohr pooled. [b] Reference 29. [c] Present work. [d] Reference 40.

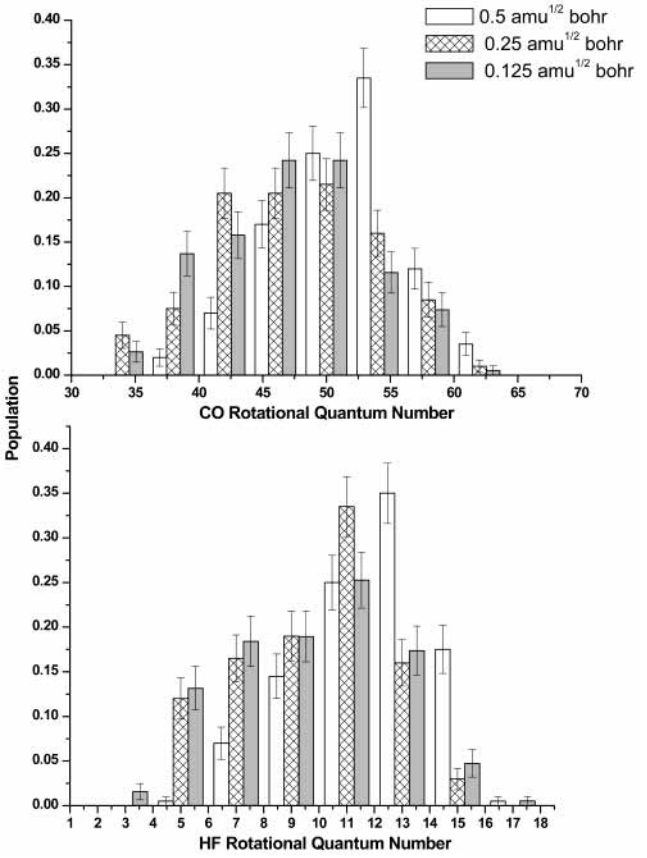

Figure 3. Rotational populations for CO and HF computed at MP2/6-31G(d,p) at three different step sizes.

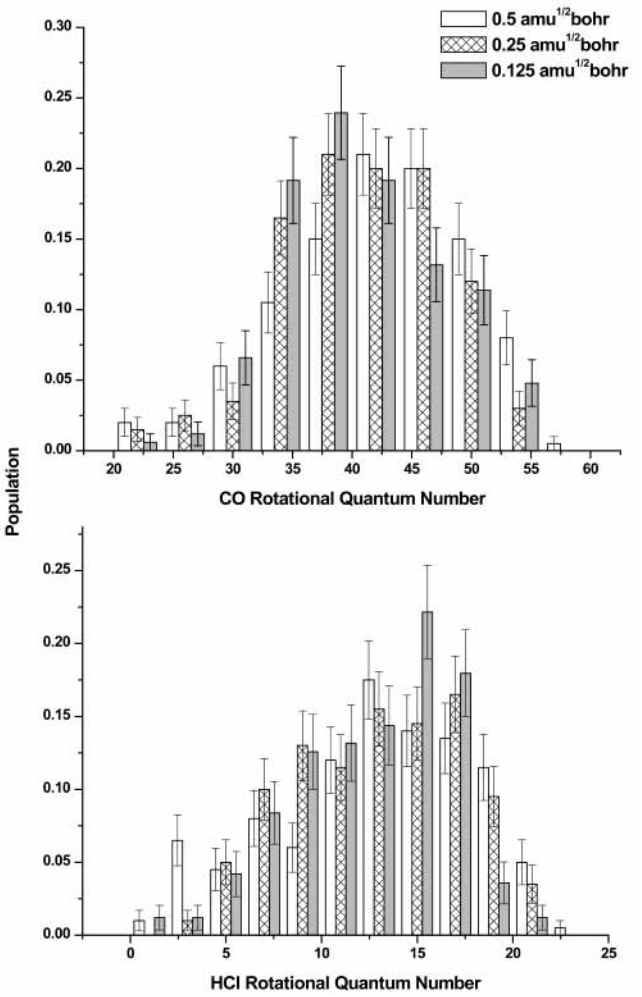

Figure 4. Rotational populations for CO and HCl computed at MP2/6-31G(d,p) at three different step sizes.

$= 0.5$ amu$^{1/2}$ bohr and at $v = 3$ for $s = 0.25$ and 0.125 amu$^{1/2}$ bohr. At the 90% confidence level, the distributions for the two smaller step sizes are the same.

Figures 3 and 4 show the effect of the step size on the product rotational distributions for HFCO and HClCO dissociation. The widths of the distributions are similar, but the means vary with the step size. For HFCO, the average rotational quantum numbers are 51.1, 47.1, and 46.6 for CO and 11.8, 9.6, and 9.4 for HF at step sizes of 0.5, 0.25, and 0.125 amu$^{1/2}$ bohr, respectively. Likewise, for HClCO, $\langle J_{CO} \rangle = 42.2$, 40.9, and 40.5 and $\langle J_{HCl} \rangle = 12.8$, 12.9, and 12.6, respectively. As with the vibrational populations, the rotational distributions obtained with $s = 0.25$ and 0.125 amu$^{1/2}$ bohr are statistically equivalent at the 90% confidence level. Since both the vibrational and rotational distributions are the same at the two smaller step sizes, we have pooled the results to obtain smaller standard deviations for the discussion of the dynamics.

Comparison of Dynamics. The distributions of the rotational populations for CO and HX obtained from the trajectory calculations are shown in Figure 5. For H_2CO, HFCO, and HClCO, the average rotational quantum numbers $\langle J \rangle$ for CO are 46, 47, and 41, respectively (corresponding to an average energy of about 11, 12, and 9 kcal/mol, respectively).[24,29] In all three molecules, the CO fragment shows a similar rotational distribution. The rotational distribution for the HX fragments is narrower and the average quantum numbers are much smaller than for CO. As the HX fragment becomes heavier (from H_2 to HF to HCl), its rotational distribution becomes broader and $\langle J \rangle$ increases: 3.3 for H_2, 9.5 for HF, and 12.8 for HCl (corresponding to an average energy of about 4.1, 6.3, and 6.5 kcal/mol, respectively).[24,29] In formyl fluoride, about 22% of the available energy is partitioned into CO rotation compared to only about 12% in HF rotation. The calculated CO rotational-energy partitioning agrees well with the experimental value of 20%.[34] In the formyl chloride case, 18% of the energy goes into CO rotation, and 12%, into HCl rotation.

The product vibrational distributions for the three reactions are compared in Table 8. The results for H_2CO have been discussed previously and are in good agreement with experi-

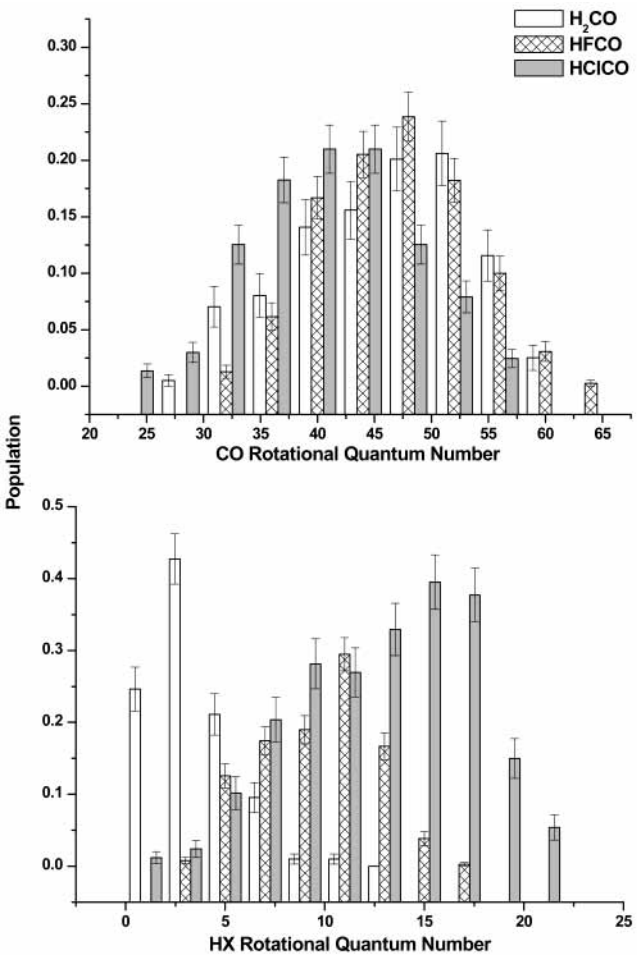

Figure 5. Rotational distributions for CO and HX computed at the MP2 level of theory.

ment. The calculations on formyl fluoride show that HF has a significant amount of vibrational excitation with an average vibrational energy of 11.4 kcal/mol. These results are in good agreement with the observations of the IRMPD studies by Ishikawa et al.[44] and the studies by Klimek and Berry.[55] However, there are no direct observations of the HF vibrational-energy distribution. In agreement with experiments[34] and previous calculations,[40] no CO was observed in $v \geq 2$ states-during the dissociation of HFCO. For HClCO, there are no experimental or computational data available for comparison. The average vibrational energy of HCl is calculated to be 20 kcal/mol, corresponding to an average quantum number of $\langle v \rangle = 2.3$. The energy deposited in HCl vibration is significantly greater than for HF, despite the fact that the energy release and the percent bond elongation for HX in the transition state are very similar for both HFCO and HClCO.

In the dissociation of HFCO, the average translational energy of the CO fragments is calculated to be 9.4 kcal/mol, and that of the HF fragments is 13.2 kcal/mol. Thus, about 42% of the available energy goes into product translation during the dissociation. This agrees well with the experiment[34] and previous theoretical calculations.[40] During the dissociation of HClCO, about 31% of the available energy is calculated to go into product translation (9.1 kcal/mol for CO and 7.1 kcal/mol for HCl).

Conclusion

Direct classical trajectories for the unimolecular dissociation of HXCO have been computed at the MP2/6-31G(d,p) level of theory. The product energy distributions are affected by the step size. Values of 0.25 and 0.125 amu$^{1/2}$ bohr produce statistically equivalent distributions, but 0.5 amu$^{1/2}$ bohr is too large and gives inaccurate results, especially for HF. With smaller step sizes, the results show good qualitative agreement with the available experimental observations. The product translation in the dissociation of HFCO receives about 42% of the available energy, which is in good agreement with the experiment. For both HFCO and HClCO, the rotational and vibrational energy distribution for CO is similar to that seen in the photodissociation of formaldehyde. The CO is produced primarily in $v = 0$, with 10−20% in $v = 1$ and none in $v = 2$. The rotational distributions are broad and peak in the range of $J = 40-50$. The average vibrational quantum numbers calculated for HCl ($\langle v \rangle = 2.3$) are significantly larger than for HF ($\langle v \rangle = 1.0$) or H_2 ($\langle v \rangle = 1.16$). The average rotational quantum number is calculated to be $\langle J \rangle = 12.8$ for HCl, which is higher than $\langle J \rangle = 9.5$ for HF, which in turn is higher than $\langle J \rangle = 3.3$ for H_2. Comparing the dissociation of HFCO and HClCO to that of H_2CO, since HF and HCl are respectively about 10 and 18 times heavier than H_2, a smaller fraction of the available energy goes into product translation (70% in H_2CO vs 42% in HFCO vs 31% in HClCO), and more goes into CO rotation (13% in H_2CO vs 22% in HFCO vs 18% in HClCO) and HX vibration (16% in H_2 vs 22% in HF vs 39% in HCl). There are no experimental or theoretical data available on the dynamics of the molecular dissociation of HClCO. Our present trajectory calculations provide the first theoretical description of the dissociation dynamics of HClCO, and the predicted results should be similar in quality to our calculations on H_2CO and HFCO.

Acknowledgment. This work was supported by grant a from the National Science Foundation (CHE 0131157). We thank C&IT and ISC at Wayne State University for computer time.

References and Notes

(1) Houston, P. L.; Moore, C. B. *J. Chem. Phys.* **1976**, *65*, 757.
(2) Ho, P.; Bamford, D. J.; Buss, R. J.; Lee, T. T.; Moore, C. B. *J. Chem. Phys.* **1982**, *76*, 3630.
(3) Moore, C. B.; Weisshaar, J. C. *Annu. Rev. Phys. Chem.* **1983**, *34*, 1664.
(4) Debarre, D.; Lefrebvre, M.; Péalat, M.; Taran, J.-P. E. *J. Chem. Phys.* **1985**, *83*, 4476.
(5) Bamford, D. J.; Filseth, S. V.; Foltz, M. F.; Hepburn, J. W.; Moore, C. B. *J. Chem. Phys.* **1985**, *82*, 3032.
(6) Guyer, D. R.; Polik, W. F.; Moore, C. B. *J. Chem. Phys.* **1986**, *84*, 6519.
(7) Butenhoff, T. J.; Carleton, K. L.; Chuang, M. C.; Moore, C. B. *J. Chem. Soc., Faraday Transactions 2* **1989**, *85*, 1155.
(8) Polik, W. F.; Guyer, D. R.; Moore, C. B. *J. Chem. Phys.* **1990**, *92*, 3453.
(9) Butenhoff, T. J.; Carleton, K. L.; Moore, C. B. *J. Chem. Phys.* **1990**, *92*, 377.
(10) Carleton, K. L.; Butenhoff, T. J.; Moore, C. B. *J. Chem. Phys.* **1990**, *93*, 3907.
(11) Butenhoff, T. J.; Carleton, K. L.; vanZee, R. D.; Moore, C. B. *J. Chem. Phys.* **1991**, *94*, 1947.
(12) van Zee, R. D.; Pibel, C. D.; Butenhoff, T. J.; Moore, C. B. *J. Chem. Phys.* **1992**, *97*, 3235.
(13) van Zee, R. D.; Foltz, M. F.; Moore, C. B. *J. Chem. Phys.* **1993**, *99*, 1664.
(14) Goddard, J. D.; Schaefer, H. F. *J. Chem. Phys.* **1979**, *70*, 5117.
(15) Harding, L. B.; Schlegel, H. B.; Krishnan, R.; Pople, J. A. *J. Phys. Chem.* **1980**, *84*, 3394.
(16) Adams, G. F.; Bent, G. D.; Bartlett, R. J.; Purvis, G. D. *J. Chem. Phys.* **1981**, *75*, 834.
(17) Goddard, J. D.; Yamaguchi, Y.; Schaefer, H. F. *J. Chem. Phys.* **1981**, *75*, 3459.
(18) Dupuis, M.; Lester, W. A.; Lengsfield, B. H.; Liu, B. *J. Chem. Phys.* **1983**, *79*, 6167.
(19) Frisch, M. J.; Binkley, J. S.; Schaefer, H. F. *J. Chem. Phys.* **1984**, *81*, 1882.

(20) Troe, J. *J. Phys. Chem.* **1984**, *88*, 4375.
(21) Scuseria, G. E.; Schaefer, H. F. *J. Chem. Phys.* **1989**, *90*, 3629.
(22) Miller, W. H.; Hernandez, R.; Handy, N. C.; Jayatilaka, D.; Willetts, A. *Chem. Phys. Lett.* **1990**, *172*, 62.
(23) Chang, Y. T.; Minichino, C.; Miller, W. H. *J. Chem. Phys.* **1992**, *96*, 4341.
(24) Chen, W.; Hase, W. L.; Schlegel, H. B. *Chem. Phys. Lett.* **1994**, *228*, 436.
(25) Peslherbe, G. H.; Hase, W. L. *J. Chem. Phys.* **1996**, *104*, 7882.
(26) Nakano, H.; Nakayama, K.; Hirao, K.; Dupuis, M. *J. Chem. Phys.* **1997**, *106*, 4912.
(27) Feller, D.; Dupuis, M.; Garrett, B. C. *J. Chem. Phys.* **2000**, *113*, 218.
(28) Song, B. J.; Kim, M. S. *J. Chem. Phys* **2000**, *113*, 3098.
(29) Li, X.; Millam, J. M.; Schlegel, H. B. *J. Chem. Phys.* **2000**, *113*, 10062.
(30) Choi, Y. S.; Moore, C. B. *J. Chem. Phys.* **1989**, *90*, 3875.
(31) Choi, Y. S.; Moore, C. B. *J. Chem. Phys.* **1991**, *94*, 5414.
(32) Choi, Y. S.; Moore, C. B. *J. Chem. Phys.* **1992**, *97*, 1010.
(33) Choi, Y. S.; Teal, P.; Moore, C. B. *J. Opt. Soc. Am. B* **1990**, *7*, 1829.
(34) Choi, Y. S.; Moore, C. B. *J. Chem. Phys.* **1995**, *103*, 9981.
(35) Goddard, J. D.; Schaefer, H. F. *J. Chem. Phys.* **1990**, *93*, 4907.
(36) Francisco, J. S.; Zhao, Y. *J. Chem. Phys.* **1992**, *96*, 7587.
(37) Kamiya, K.; Morokuma, K. *J. Chem. Phys.* **1991**, *94*, 7287.
(38) Morokuma, K.; Kato, S.; Hirao, K. *J. Chem. Phys.* **1980**, *72*, 6800.
(39) Wei, T.-G.; Wyatt, R. E. *J. Phys. Chem.* **1993**, *97*, 13580.
(40) Yamamto, T.; Kato, S. *J. Chem. Phys.* **1997**, *107*, 6114.
(41) Yamamto, T.; Kato, S. *J. Chem. Phys.* **1998**, *109*, 9783.
(42) Yamamto, T.; Kato, S. *J. Chem. Phys.* **2000**, *112*, 8006.
(43) Saito, K.; Kuroda, H.; Nakumoto, T.; Munechika, H.; Murakami, I. *Chem. Phys. Lett.* **1985**, *113*, 399.
(44) Ishikawa, Y.; Sugita, K.; Arai, S. *Chem. Phys. Lett.* **1984**, *109*, 264.
(45) Fang, W.-H.; Liu, R.-Z. *J. Chem. Phys.* **2001**, *115*, 5411.
(46) Budenholzer, F. E.; Yu, T. *J. Phys. Chem. A* **1998**, *102*, 947.
(47) Glukhovstev, M. N.; Bach, R. D. *J. Phys. Chem. A* **1997**, *101*, 3574.
(48) Bent, G. D.; Rasmany, M.; Hall, T. *Mol. Phys.* **1994**, *82*, 825.
(49) Fang, W.-H.; Liu, R.-Z. *J. Chem. Phys.* **2001**, *115*, 10431.
(50) Wallington, T. J.; Hurley, M. D.; Ball, J. C.; Kaiser, E. W. *Environ. Sci. Technol.* **1992**, *26*, 1318.
(51) Nikki, H.; Maker, P. D.; Breitenbach, L. P.; Martinez, R. I.; Herron, J. T. *J. Phys. Chem.* **1982**, *86*, 1858.
(52) Fisher, D. A.; Hales, C. H.; Filkin, D. L.; Ko, M. K. W.; Sze, N. D.; Connell, P. S.; Wuebbles, D. J.; Isaksen, I. S. A.; Stordal, F. *Nature (London)* **1990**, *344*, 508.
(53) Ravishankara, A. R.; Turnipseed, A. A.; Jenson, N. R.; Barrone, S.; Mills, M.; Howard, C. J.; Solomon, S. *Science (Washington, D.C.)* **1994**, *263*, 71.
(54) Wallington, T. J.; Schneider, W. F.; Sehested, J.; Neilsen, O. J. *Faraday Discuss. Chem. Soc.* **1995**, *100*, 55.
(55) Klimek, D. E.; Berry, M. J. *Chem. Phys. Lett.* **1973**, *20*, 141.
(56) Bolton, K.; Hase, W. L.; Peslherbe, G. H. Direct Dynamics Of Reactive Systems. In *Modern Methods for Multidimensional Dynamics Computation in Chemistry*; Thompson, D. L., Ed.; World Scientific: Singapore, 1998; p 143.
(57) Frisch, M. J.; Trucks, G. W.; Schlegel, H. B.; Scuseria, G. E.; Robb, M. A.; Cheeseman, J. R.; Montgomery, J. A., Jr.; Vreven, T.; Kudin, K. N.; Burant, J. C.; Millam, J. M.; Iyengar, S.; Tomasi, J.; Barone, V.; Mennucci, B.; Cossi, M.; Scalmani, G.; Rega, N.; Petersson, G. A.; Ehara, M.; Toyota, K.; Hada, M.; Fukuda, R.; Hasegawa, J.; Ishida, M.; Nakajima, T.; Kitao, O.; Nakai, H.; Honda, Y.; Nakatsuji, H.; Li, X. S.; Knox, J. E.; Hratchian, H. P.; Cross, J. B.; Adamo, C.; Jaramillo, J.; Cammi, R.; Pomelli, C.; Gomperts, R.; Stratmann, R. E.; Ochterski, J.; Ayala, P. Y.; Morokuma, K.; Salvador, P.; Dannenberg, J. J.; Zakrzewski, V. G.; Dapprich, S.; Daniels, A. D.; Strain, M. C.; Farkas, O.; Malick, D. K.; Rabuck, A. D.; Raghavachari, K.; Foresman, J. B.; Ortiz, J. V.; Cui, Q.; Baboul, A. G.; Clifford, S.; Cioslowski, J.; Stefanov, B. B.; Liu, G.; Liashenko, A.; Piskorz, P.; Komaromi, I.; Martin, R. L.; Fox, D. J.; Keith, T.; Al-Laham, M. A.; Peng, C. Y.; Nanayakkara, A.; Challacombe, M.; Gill, P. M. W.; Johnson, B.; Chen, W.; Wong, M. W.; Andres, J. L.; Gonzalez, C.; Head-Gordon, M.; Replogle, E. S.; Pople, J. A. Gaussian 01 (development version); Gaussian Inc.: Pittsburgh, PA, 2002.
(58) Moller, C.; Plesset, M. S. *Phys. Rev.* **1934**, *46*, 618.
(59) Becke, A. D. *J. Chem. Phys.* **1993**, *98*, 1372.
(60) Becke, A. D. *J. Chem. Phys.* **1993**, *98*, 5648.
(61) Lee, C.; Yang, W.; Parr, R. D. *Phys. Rev. B* **1988**, *37*, 785.
(62) Pople, J. A.; Head-Gordon, M.; Raghavachari, K. *J. Chem. Phys.* **1987**, *87*, 5968.
(63) Montgomery, J. A.; Ochterski, J. W.; Peterson, G. A. *J. Chem. Phys.* **1994**, *101*, 5900.
(64) Gonzalez, C.; Schlegel, H. B. *J. Chem. Phys.* **1989**, *90*, 2154.
(65) Gonzalez, C.; Schlegel, H. B. *J. Phys. Chem.* **1990**, *94*, 5523.
(66) Millam, J. M.; Bakken, V.; Chen, W.; Hase, W. L.; Schlegel, H. B. *J. Chem. Phys.* **1999**, *111*, 3800.
(67) Bakken, V.; Millam, J. M.; Schlegel, H. B. *J. Chem. Phys.* **1999**, *111*, 8773.
(68) Hase, W. L. Classical Trajectory Simulations: Final Conditions. In *Encyclopedia of Computational Chemistry*; Schleyer, P. v. R.; Allinger, N. L.; Clark, T.; Gasteiger, J.; Kollman, P. A.; Schaefer, H. F.; Schreiner, P. R., III, Eds.; Wiley & Sons: New York, 1998; p 399.
(69) LeBlanc, O. H., Jr.; Laurie, V. W.; Gwinn, W. D. *J. Chem. Phys.* **1960**, *33*, 598.
(70) Davis, R. W.; Gerry, M. C. L. *J. Mol. Spectrosc.* **1983**, *97*, 117.
(71) *NIST-JANAF Themochemical Tables*, 4th ed.; Chase, M. W., Jr., Ed.; American Chemical Society: Washington, DC, 1998.